International Journal of Theoretical & Applied Sciences, 9(2): 11-24(2017)

ISSN No. (Print): 0975-1718
ISSN No. (Online): 2249-3247

Ag^{+9} Swift Heavy ion Irradiation: Augmented Removal of auramine-O Dye and Bactericidal Activity

Sukriti, B. S. Kaith and Rajeev Jindal
Department of Chemistry,
Dr B.R. Ambedkar National Institute of Technology, Jalandhar, (Punjab), India.

(Corresponding author: Sukriti)
(Received 02 July, 2017 accepted 05 August, 2017)
(Published by Research Trend, Website: www.researchtrend.net)

ABSTRACT: Present work is concerned with synthesis of semi-interpenetrating network based on *Gum xanthan* graft co-polymerized with polyacrylic acid in presence of glutaraldehyde-ammonium persulfate as cross linker-initiator system. Different reaction parameters were optimized in order to incorporate maximum fluid uptake efficacy. Further the sample is irradiated with 120 M eV Ag^{+9} swift heavy ion(SHI) with the fluence of 2 $\times 10^{12}$ ions cm^{-2} and low current of 1.0 pnA. Structural and morphological changes undergone by the sample on irradiation was studied using various techniques like FT-IR, SEM-EDX and XRD. Irradiated sample was further tested as an adsorbent for the sequestration of auramine-O dye and its dye adsorption potential increases upto 78.62%. Further, the enhanced bactericidal activity of the irradiated samples was observed against *Bacillus subtilis*, *Staphylococcus aureus, Escherichia coli* and *Salmonella enteritis*. Therefore, Ag^{+9} SHI irradiated sample can be used effectively as a dye adsorbent and bactericidal agent with good efficiency.

Keywords: Gum xanthan; semi-interpenetrating network; swift heavy ion; auramine-O; antibacterial

I. INTRODUCTION

Hydrogels are regarded as a special class of superabsorbents formed by the graft co-polymerization of long polymeric chains onto natural or synthetic polymer backbone which were further chemically or physically crosslinked to impart dimensional stability. The 3D cross linked network formed had tremendous potential to imbibe aqueous fluid thousand times of its weight without itself dissolving in it [1]. Some of the natural and synthetic polymers which are used exclusively are *Gum ghatti*, gelatin, collagen, *guar gum*, alginate, chitosan, dextran, hyaluronic acid and poly (vinyl alcohol), poly(lactic acid) and poly(ethylene glycol) [2,3]. The natural polymer generally had a poor mechanical strength while synthetic polymers were non-biodegradable in nature so, the pros and cons of both the natural and synthetic polymers could be combat together by graft copolymerization to tailor the 3D polymeric network depending upon its further applicability in various fields [4].

Gum xanthan a natural high molecular weight polysaccharide with branched side chains and acidic characteristic. It is secreted by the *Xanthomonas campestris* bacteria under aerobic conditions through fermentation of glucose, sucrose or with complex substrate like molasses, sugar cane, corn or their derivatives [5-7]. It was a complex polysaccharide consisting of a primary chain of β-D-(1, 4)-glucose backbone along with a trisaccharide side chain on every other glucose at C-3, containing a glucuronic acid residue linked (1 → 4) to a terminal mannose unit and (1→2) to a second mannose that connects to the backbone. The presence of both glucuronic acid and pyruvic acid was mainly responsible for the anionic character of *Gum xanthan* [8].

The surface properties without affecting bulk properties of the polymeric materials can be modified using various techniques such as laser, plasma, chemical etching, electron beam and ion beam irradiation [9-10]. Ion beam irradiation due to its intense electronic energy deposition brought the columnar defects, point defects and amorphous tracks along its path owing to the material modification in more efficient and precise manner. The properties of the material are tailored upon irradiation due to triggered chemical transformations such as chain scission, new bond formation, generation of volatile moieties and appearance of extensive crosslinks [11,12]. It is well documented in the literature that ion beam irradiation resulted into appreciable improvement in the chemical, electrical, optical, thermal and dielectric properties of the exposed material.

The extent and type of modification in the material depends upon the type, energy and intensity of ion beam used [13, 14]. The bactericidal characteristic of silver is known since ages and it has been found effective against broad spectrum of microbes. Due the effectivity of the silver ions in controlling the growth of microbes, it is extensively used in medicinal and pharmaceutical sectors. It also finds wide application in the field of disinfectants, wound dressings, cosmetics, textile coatings and electrical appliances [15-17]. Jayaramudu *et al.* (2013) has reported the excellent antimicrobial activity of Iota-Carrageenan based on biodegradable silver nanocomposite hydrogels [18]. Jain *et al*. (2005) have fabricated the silver nanoparticle-coated polyurethane foam and utilized it as an antibacterial water filter [19].

Water pollution is undoubtedly the most hazardous form of pollution as it disturbs not only the aquatic systems, but is also harmful for humans. Major water pollutants include heavy metals, dyes, sediments, fluorides, and toxic chemicals containing nitrates and phosphates, radioactive pollutants, and the wastes from pharmaceuticals and personal care products [20, 21]. Apart from these, dyes have played the major havoc due to their great solubility in water along with creating unsightly appearance. Dye metabolites formed upon degradation are toxic, mutagenic, carcinogenic and potentially teratogenic in nature. Therefore, they severely influence the ecosystem and ultimately effects the complete biosphere which is inter-liked by food web [22].

Auramine-O (4,4'-dimethylaminobenzophenonimide) is a cationic dye which is used extensively in the paper, textiles and leather industries as a coloring material [23]. There are many kinds of technologies used for the removal of dyes from wastewater such as membrane separation, chemical oxidation, coagulation, photocatalytic degradation and adsorption methods [24]. Nowadays adsorption is the most common technology for the removal of dyes from wastewater due to its effectiveness, efficiency, economy and lack of associated secondary pollution. Many non-conventional low-cost adsorbents including natural materials, biosorbents, polymeric materials, and waste materials from industry and agriculture are used for dye removal [25].

Present works deals with modification of the physical and chemical characteristics of the *Gum xanthan* based superabsorbent on irradiation with the Ag^{+9} swift heavy ions (SHIs). Further, the influence of SHIs on antibacterial and dye uptake potential of the irradiated sample is explored.

II. EXPERIMENTAL

A. Material and methods

Gumxanthan was purchased from Sigma Aldrich. Acrylic acid, acrylamide, glutaraldehyde and Auramine-O (Aur-O) were obtained from Merck, India Ltd. Peptone, beef extract, NaCl and agar were procured from Hi-media Ltd. Bacterial strains were received from CRI, Kasuli H.P. All the chemical were of analytical grade and used without further purifications. All the solutions were prepared in double distilled water.

B. Synthesis of Gx-cl-poly(AA)-IA

In typical experiment, 1.0 g of *Gum xanthan* was dissolved in known amount of double distilled water with continuous stirring till uniform lump free slurry was obtained. It was followed by the drop-wise addition of acrylic acid to the reaction mixture with constant stirring. Calculated amount of glutaraldehyde and ammonium per sulfate were added with vigorous stirring to the resulting mixture. The subsequent reaction was carried out at a specific temperature and time duration. The resulting product was freed from homopolymer through solvent extraction using distilled water. The final product was dried at 65˚C till constant weight was obtained. Different reactions parameters such as reaction time, reaction temperature, pH of reaction medium, initiator concentration, monomer concentration, cross-linker concentration and solvent volume were optimized with respect to maximum percentage swelling (P_s).

The percentage swelling was determined by taking a known weight of the dried sample obtained and was kept in distilled water for 24 h at room temperature. The residual water molecules adhered to the surface of swollen sample were removed gently with filter paper and weighed after regular intervals till equilibrium was attained. The percentage swelling (P_s) was calculated as per Eq. 1[26]:

$$P_S = \frac{W_S - W_d}{W_d} \times 100 \qquad (1)$$

where, P_s = percentage swelling; W_s = weight of swollen sample; W_d = weight of dry sample.

The replications were carried out in triplicate for the reproducibility of the results and statistical analysis was performed using Microsoft Excel 2010.

C. Swift heavy ion irradiation

Swift heavy ions (SHIs) are the high energy radiations with energy ranging from KeV to GeV were employed extensively for the modification of chemical and physical characteristics of the materials depending upon the requirement.

They impinge into the material and exchange its high energy either by elastic collision with the nuclei of target atoms or by triggering the ionization of the atoms due to inelastic collision [27, 28]. The facility of ion beam irradiation was availed at Inter University Accelerator Centre (IUAC), New Delhi, India. The 15 UD pelletron which was used as platform for SHIs irradiation act as a versatile electrostatic accelerator which produces negative ions. The ions were pre-accelerated to ~300KeV in ion source and transferred *via* accelerating tubes to the accelerator tank with a strong electrical field maintained inside and filled with SF_6 insulating gas. After traversing the terminal shell maintained at high voltage of ~15 MV, the negative ions pass through stripper which extracts some electrons and transform them into positive ions. The positive ions formed were repelled by the positively charged terminal shell and were accelerated to the ground potential to the bottom of the tank. The analyzing magnet present at the end of the tank select the particular ion beam along with bending of the ions into horizontal planes. Further, the switching magnet diverts the different swift heavy ion beams generated into various beam lines which were used for material modifications. The entire machine was computerized which could be easily operated from the control room. The type of ions and its energy could be selected according to the degree of modification in the material under investigation. In the present study the synthesized hydrogel was irradiated with 120 M eV Ag^{+9} SHI with the fluence of 2×10^{12} ions cm^{-2} and low current of 1.0 pnA was used to avoid thermal degradation of polymeric samples in material science lab with 15 UD pelletron IUAC, New Delhi. The beam was moved continuously in XY plane onto the sample to impose the uniform surface modification. The irradiation time was calculated using Eq. 2 [27]:

$$t = \frac{\emptyset Aqe}{I} \qquad (2)$$

Where, ∅ is the fluence (ions cm^{-2}), A is irradiation area of the sample (cm^{-2}), *I* is the current (pnA).

The candidate polymer was exposed to Ag^{+9} swift heavy ion and undergoes remarkable change in physical and chemical properties which was confirmed by FT-IR, FE-SEM and XRD. Irradiated sample was further tested for improved dye removal potential from aqueous solution and enhanced antibacterial activity.

D. Instrumentation

To evaluate the changes imposed in the sample upon irradiation with Ag^{+9} swift heavy ion, the sample was characterized before and after irradiation by various techniques. FT-IR spectra was perceived from Carry 630 spectrophotometer, Agilent Technologies with diamond crystal in the range of 4000-400 cm^{-1}. X-ray diffraction studies was carried out using Bruker AXS, X-ray diffractometer. Micrographs of Scanning Electron Microscopy-Energy Dispersive X-Ray Spectroscopy (SEM-EDX) for determining the morphological changes and elemental constitution were obtained using JEOL JSM-6490LV microscope at 10 kV with platinum coating. The absorbance spectra for dye uptake studies was obtained using Agilent Technologies Carry 631 UV-Vis Spectrophotometer. The weighing were performed on CPA225D Sartorius analytical balance.

E. Dye removal

The adsorption experiment on the cationic dye, auramine-O (Aur-O) using Gx-cl-poly(AA)-IA pristine and Ag^{+9} irradiated samples was carried out using batch mode. The experiment set up involves 100 mg sample placed in 40ml (30ppm) of both Aur-O dye solution. The change in the concentration of the residual dye solution upon advent of adsorption by the sample was noted after every 30 mins for the time duration of 5 h which was analyzed using UV-VIS spectrophotometer at 434.8 nm λ_{max}. The percentage removal of the dye was calculated as per the Eq. 3 [29]:

$$\%\, Dye\ Removal = \frac{C_o - C_e}{C_o} \times 100 \qquad (3)$$

Where C_o = initial dye concentration (mg L^{-1}) and C_e (mg L^{-1}) = residual dye concentration upon adsorption.

F. Antibacterial activity

Antibacterial activity was carried out using Agar-Well Diffusion method [30]. For the preparation of plates, nutrient agar medium was prepared by dissolving peptone (5.0 g), beef extract (3.0 g), NaCl (5.0g) and agar (20.0g) in 1000 ml of distilled water with constant stirring. The agar medium obtained was sterilized in autoclave at a pressure of 15 lbs for 60 mins. 20-25 ml of this medium was transferred to each sterilized petri plate in laminar flow and allowed to solidify for 24 h. For the activation of bacteria, 5ml of nutrient broth was transferred to 4 separate test tubes after sterilization and inoculum of 4 different bacterial strains such as *Bacillus subtilis*, *Staphylococcus aureus, Escherichia coli* and *Salmonella enteritis* collected from CRI, Kasuli were added respectively. After 24 h of incubation 100µl of each bacteria was taken and swabbing was done on the prepared plates with sterilized swaps. Wells of 7mm in diameter was made with cork borer under sterilized conditions. To each prepared wells 40mg/ml of sample was added. Amoxicillin was used as a control. The plates were incubated at the temperature of 28 ± 2°C for 24 h after which the zone of inhibition appeared.

The antibacterial activity of the samples directly corresponds to the diameter of zone of inhibition against different bacteria. The diameter of zone of inhibition for the candidate polymer before and after irradiation with Ag^{+9} SHI, along with control was recorded to determine the impact on the antibacterial activity of the sample.

III. RESULTS AND DISCUSSION

The synthesis of semi-interpenetrating network in-air condition proceeded *via* free radical chain polymerization reaction. Formation of 3 D polymeric network involves the grafting of long polyacrylic acid chains onto *Gum xanthan* which was further crosslinked by glutaraldehyde for structural rigidity. Firstly, the initiation step involves the decomposition of ammonium persulphate used as thermal initiator which resulted into generation of pair of sulphate radical-anion. SO_4^{-*} further dissociates H_2O molecules (solvent) and generates OH^* and HSO_4^-. SO_4^{-*} and OH^* together generate brigade of new radical centers on –OH and $–CH_2$ functional groups present on backbone and monomer (acrylic acid) moieties respectively. Live polyacrylic acid chains got graft copolymerized onto activated centers appeared on backbone along with crosslinking through glutaraldehyde. The propagation of chain reaction continues till the homopolymerzation (coupling reaction) dominated the graft copolymerization which ultimately leads to termination of the reaction. The chain reaction may also seize upon disproportionate reaction which involves simultaneous oxidation and reduction of activated monomeric moieties resulting into formation of alkene and alkane moieties [29].

A. Optimization of reaction parameter

In order to obtainGx-cl-poly(AA)-IA with maximum fluid efficacy (410.3%) the various process parameters were optimized with respect to swelling percentage (Eq.1). The parameters optimized were APS = 8.7×10^{-3} mol L^{-1}; reaction time = 210 secs; solvent = 20 mL; reaction temperature = 60 °C; acrylic acid = 2.91mol L^{-1}; glutaraldehyde = 2.6 mol L^{-1} and pH = 7.0 (Figs. 1a-g).

The effect of initiator concentration on maximum fluid efficacy (P_s) was estimated by varying the concentration from 6.5×10^{-3} to 15.3×10^{-3} mol L^{-1}. P_s was found to increase slowly with increase in the initiator concentration and tends to attain maximum value at 8.7×10^{-3} mol L^{-1} (P_s = 230.19 %). Further increase in the initiator concentration leads to decrease in P_s. Increase in P_s at lower initiator concentration was attributed to generation of optimum amount of radical sites on backbone and monomer moieties which resulted into rapid graft copolymerization. While at higher initiator concentration large number of active radical sites were created which leads to dominance of homopolymerzation instead of graft copolymerization and resulted into termination of the chain process thereby shortening the polymer chain length and along with free volume available within the matrix which was ultimately responsible for decreasing P_s [31](Fig. 1a).

Reaction time and temperature also played significant role in synthesizing semi-IPN with good fluid retaining ability. With increase in reaction time (150-270 sec) and temperature (55-75°C) P_s was increased and attained maximum value of 296.38% (210 sec) and 368.98 % (60°C) respectively, beyond this point prominent decrease in fluid uptake efficacy of candidate polymer was observed (Fig. 1b and Fig. 1c). After attainment of optimum time decrease in P_s was observed due to intensive grafting of polyacrylic acid chains onto backbone along with excessive crosslinking which results into rigid and compact structure owing to decreased P_s. While decrease in P_s with increasing temperature beyond optimum value was probably due to faster chain termination and chain transfer reaction along with scavenging of SO_4^{-*} and OH^* free radical centers with O_2 radical scavenger generated by APS due to thermal degradation at higher temperature leads to the formation lesser gel content responsible for lesser fluid uptake at higher temperature [31, 32].

Varying the solvent amount and monomer concentration also significantly influenced the swelling ability of the samples. Increasing the solvent amount from 5-25 ml and monomer concentration from 2.18-5.09 mol L^{-1} Ps was found to increase linearly and attained maximum value at 20 mL (330.95%) and 2.91 mol L^{-1} (354.23%), respectively. Initial increase in Ps on increasing the solvent amount was probably due to increased production of OH* free radicals which further triggers the generation of more radical centers on *Gum xanthan* and monomer moieties thereby promoting the propagation of chain reaction for graft polymerization. However on increasing the solvent amount reduces the generation of hydroxyl radicals which in turns produces lesser active sites and hence reduces P_s. Similarly by increasing the monomer concentration increases the availability of the hydrophilic monomer moieties in the vicinity of backbone promoting greater extent of graft copolymerization while increase in monomer concentration beyond optimum level, leads to increase in inter- and intra-molecular self-crosslinkage through secondary bonding forces which reduces the free volume available for accommodation of more solvent molecules into the polymeric matrix [33].

Structural stability to the 3D graft copolymer was provided by the chemical crosslinker. The maximum P_s was obtained at crosslinker concentration of 2.6 mol L^{-1} (398.11%) increasing the concentration beyond this was directly responsible for structural rigidity and compactness which ultimately reduces the water uptake potential of the sample.

Influence of the pH on the liquid uptake potential was observed in different pH solutions ranging from 3.0 to 11.0 prepared by diluting 0.1M HCl and NaOH solutions. Maximum P_s of 410.33% was observed at pH 7.0. Prominent decrease in Ps value was observed in both acidic and basic conditions. This can be illustrated by osmotic pressure swelling theory described in Eq. 5 [33]:

$$\pi_{ion} = RT \Sigma (C_g - C_s) \quad (5)$$

where, C_g = molar concentration of mobile ions in swollen sample; C_s = molar concentration of mobile ions in external fluid; R = universal gas constant; T = absolute temperature.

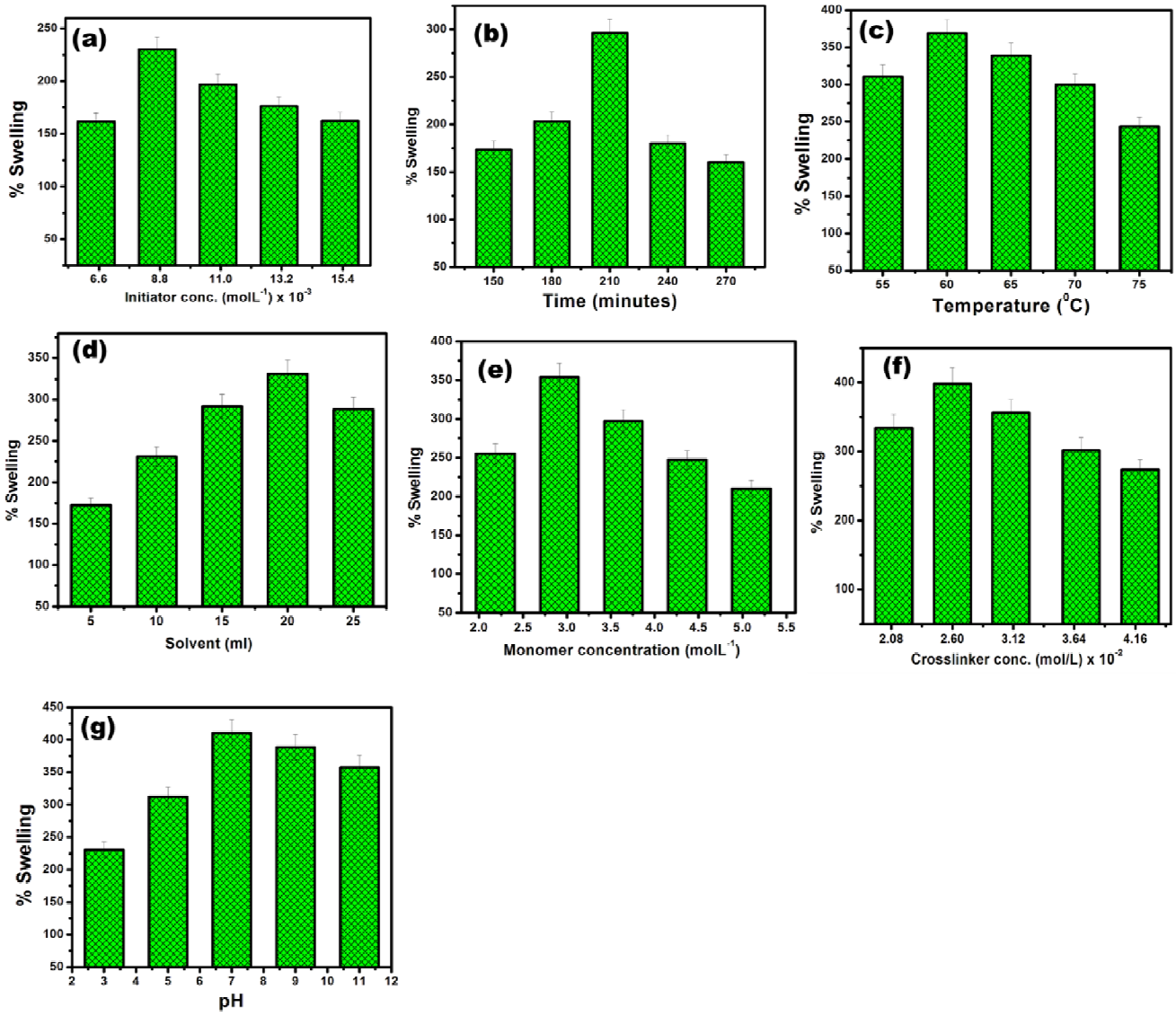

Figs. 1a-g. Variation of percentage swelling with with (a) initiator concentration; (b) time; (c) temperature; (d) solvent concentration; (e) monomer concentration; f) crosslinker concentration; (g) pH.

Gum xanthan contained numerous glucornic acid groups with $–COO^-$ moieties along with polyacrylic acid polymeric chains grafted onto it upon propagation reaction. In neutral medium, concentration of the ions in the external medium (C_s) were insignificant and hence osmotic pressure increase which further increase the inflow of solvent molecule into polymeric matrix which corresponds to increased P_s. Also, more extensive polymeric structure was formed due to repulsions between different polymeric chains of synthesized superabsorbent, possessing –COO– groups resulting in increased liquid uptake. In acidic medium, H^+ ions screened the repulsion between –COO– groups present on polymeric chains which resulted in lower value of C_g and Π_{ion}. Similarly, in basic medium, the Na^+ ions produced a screening effect between the ion repulsing chains possessing –COO– groups leading to lower C_g and Π_{ion} value. Hence, lower liquid uptake was found under acidic and basic conditions [29].

B. Characterization

X-ray diffraction. XRD pattern of Gx-cl-poly(AA)-IA before and after irradiation with Ag^{+9} SHI were recorded in the halos extending in the range of 10-60° on 2θ scale (Figs. 2a,b). The percentage crystallinity (X_c) was calculated as the ratio of crystalline area to the total area comprised of amorphous and crystalline domains as per Eq. 6 [34]:

$$Xc = \left\{\frac{Ac}{Ac+Aa}\right\} \times 100 \quad (6)$$

Where, A_c = area of crystalline phase, A_a= area of amorphous phase and X_c = percentage Crystallinity.
Further, the coherent length L (A°) representing the crystallite size was evaluated using the Scherrer equation as per Eq. 7 [27]:

$$L = \frac{0.9\lambda}{\beta \cos\theta} \quad (7)$$

Where, L = coherent length; λ=X-ray wavelength (for Cu Kα, λ = 1.541 A°); β = full width half maxima and θ = diffraction angle.

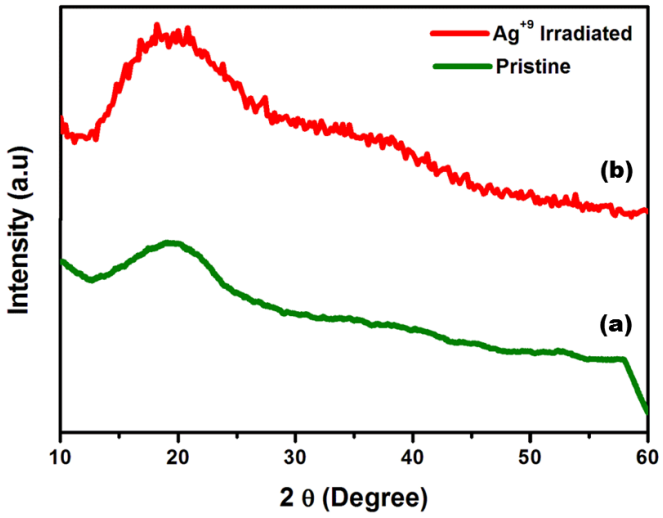

Figs. 2a-b. XRD of Gx-cl-poly(AA)-IA (a) pristine; (b) Ag^{+9} SHI irradiated.

XRD spectra of *Gum xanthan*, no characteristic peak was observed in the 2θ range extending from 10-60° indicating its highly amorphous nature [34]. However, the spectra of pristine Gx-cl-poly(AA)-IA showed the maximum peak intensity (I) at to 2θ = 20.34°(I = 81.92 a.u.) and coherent length of 2.83 A°. Also, the pristine Gx-cl-poly(AA)-IA was found to be 72.49% crystalline. The increase in relative peak intensity (I) at 2θ, coherent length (L) and % Crystallinity (X_c) for the synthesized sample confirmed the formation of 3D crosslinked network with more ordered arrangement due to induced graft co-polymerization on completely amorphous backbone with subsequent increase in crosslinking density with increased crosslinker concentration owing to enhanced coherent length which ultimately promotes anisotropy [35].
However on irradiation with Ag^{+9} SHI ions the XRD spectra of Gx-cl-poly(AA)-IA depicted significant changes. It depicted the maximum peak intensity corresponding to 2θ = 18.2° (I = 1765a.u.) and coherent length of 3.64 A°.

The percentage crystallinity for the irradiated sample was found to increase to 78.64%. It was observed that upon irradiation with Ag^{+9} SHI there was a prominent increase in peak intensities, coherence length and percentage crystallinity which directly indicated towards the enhanced crystallinity of the 3D crosslinked polymeric network upon impingement of the high energy Ag^{+9} SHI into the matrix This can be explained according to the thermal spike model according to which there was a local rise in the temperature for very short period of time along the path of the SHI ion which prompted the crystallization process into the exposed material [36, 37].

FTIR spectroscopy. FT-IR spectra of *Gum xanthan* depicted a broad hump at 3264.2 cm^{-1} (–OH stretching of carbohydrates), weak band at 2927.1 cm^{-1} (–CH_2 symmetric stretching), 1651.2 cm^{-1} (-C=O stretching for ester of pyruvate group), 1414.4 cm^{-1} (-CH_2 in plane bending),1173.7 cm^{-1} (C-O-C stretching) and 1020.1 cm^{-1} (C-O stretching vibrations) [34].

However, the FT-IR spectra of Gx-cl-poly(AA)-IA exhibited the prominent sharp peak at 1701.3 cm^{-1} for –C=O stretching for acids, in addition to the peaks already depicted in the spectra of backbone. Also, the peak around 3264.2 cm^{-1} (for –OH of carbohydrates) further broadens and shifts slightly due to incorporation of hydrogen bonded –OH moieties of the polyacrylic acid grafted chains onto the backbone (Fig. 3a).

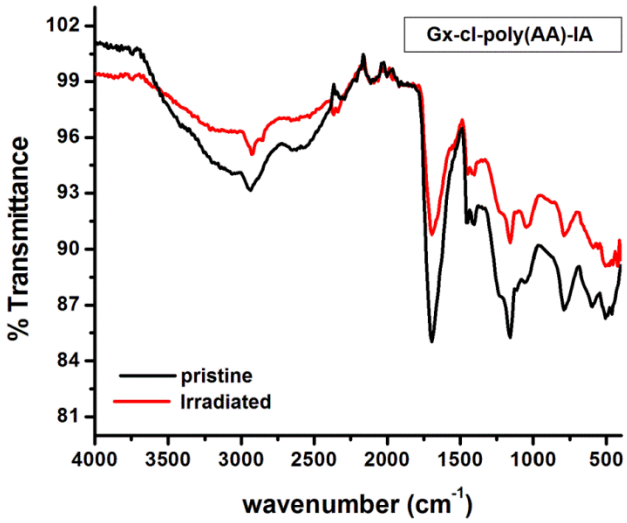

Figs. 3a,b. FT-IR spectra of Gx-cl-poly(AA)-IA (a) pristine; (b) Ag^{+9} SHI irradiated.

The chemical modifications in the irradiated samples can be determined by comparing the changes imposed on the vibration modes as evaluated by FT-IR (Fig. 3b). The FT-IR spectra of pristine and irradiated Ag^{+9} SHI were compared. It was observed that the band shape depicted slight shifting and modification upon irradiation. Most of the peaks present in pristine sample were also depicted in the irradiated samples with slight shifting and reduced intensity along with the appearance of few new peaks. Reduction in peak intensities of C-O, -C=O,-O-H and -C-H were observed in all the samples which signified that the polymeric network was transformed into hydrogen and oxygen depleted carbon networks due to the chain scission of carbonate linkage and emission of H_2, CO_2, H_2O along with other volatile moieties due to the local high temperature generated along the ion tracks formed by the passage of high energy Ag^{+9} SHI [37, 38].

SEM Analysis. The scanning electron microscope based on focused beam of high-energy electron revealing information about the surface morphology of the samples was used to analyse the changes brought about in the property profile on irradiation with Ag^{9+} ions (Figs. 4a,b). To increase the surface conductivity of polymeric material and prevention of charge accumulation on the surface upon focusing of electron beam to visualize the surface morphology the sample was pre-coated with platinum. Surface of *Gum xanthan* was smooth with homogeneity throughout [34]. Upon grafting of *Gum xanthan* with polyacrylic acid and crosslinking with glutaraldehyde the surface appeared to be highly heterogeneous with grooves and tree like projection all over the topograph (Fig. 4a).

The surface morphological changes induced in the sample on irradiation with Ag^{+9} SHI was clearly observed in the SEM micrograph. The surface appeared to be more rough with more extensive zig-zag tree like projection. Along with that small holes and fissures were also observed clearly on the micrographs recorded at the magnification of 2.00KX which were probably caused due to the passage of high energy Ag^{+9} SHI through the synthesized sample (Fig. 4b).

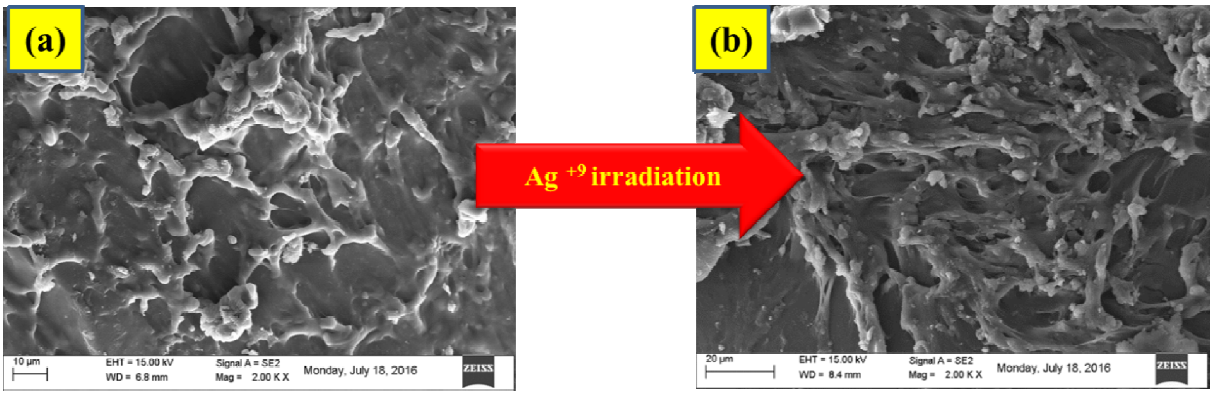

Figs. 4a,b. SEM Micrographs of Gx-cl-poly(AA)-IA (a) pristine; (b) Ag^{+9} SHI irradiated.

Electron Dispersive spectroscopic (EDS) studies. EDS was studied in conjugation of SEM and used to detect x-rays emitted from the sample characteristic to the definite element during bombardment by an electron beam under SEM analysis to evaluate the qualitative elemental composition of the test sample.

It was observed that atomic % (weight %) of carbon was 50.58% (42.92%); 58.42% (51.33%) and that of oxygen was 48.70% (55.04%), 41.58% (48.67%), in *Gum xanthan* and Gx-cl-poly(AA)-IA, respectively (Fig. 5a) [34]. The graft co-polymer synthesized clearly depicted the increase in carbon content compared to *Gum xanthan* which confirms the incorporation of vinyl monomeric chains onto polysaccharide backbone. The decrease in oxygen content was probably due to release of H_2O molecules during polymerization process of Gx-cl-poly(AA)-IA.

The presence of Ag in the spectra on irradiation of the sample confirmed the incorporation of the Ag^{+9} SHI in the pre-synthesized polymeric network. It was observed that atomic % (weight %) of 'Ag' in Gx-cl-poly(AA)-IA was 0.02% (0.19%) along with atomic percentage of 'C' and 'O' 57.09% (48.89%;) and 42.88% (49.91%), respectively (Fig. 5b).

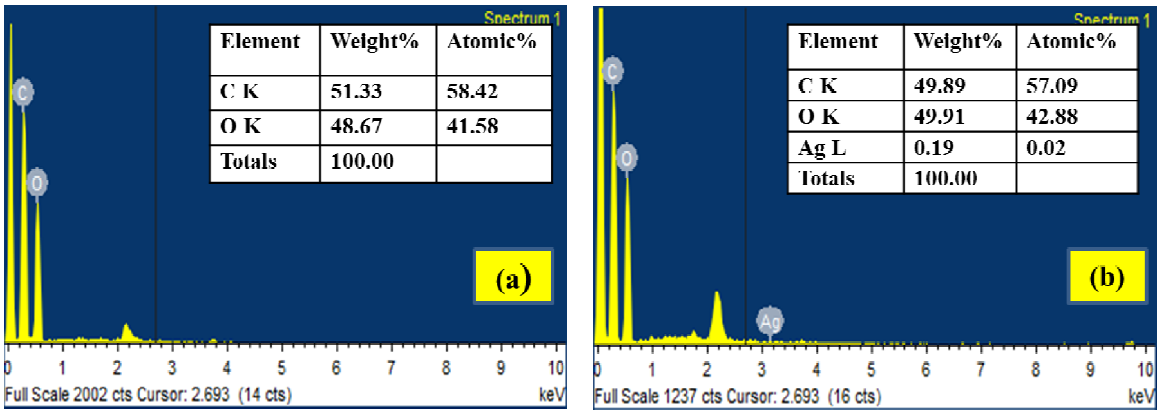

Figs. 5a,b. EDX spectra of Gx-cl-poly(AA)-IA (a) pristine; (b) Ag^{+9} SHI irradiated.

C. Antibacterial activity

The antibacterial activity of the synthesized sample was evaluated against gram-positive (*Bacillus subtilis; Staphylococcus aureus*) and gram-negative (*Salmonella enteritis; Escherichia coli*) bacteria using Agar-Well Diffusion method. It has been observed that synthesized sample was found to be quite resistant to the bacterial invasion.

The bactericidal influence was further enhanced by Ag^{+9} SHI which was confirmed by the appearance of zone of inhibition with increased diameter after 24 h of incubation (Figs. 6a-d). Control drug, amoxicillin had depicted remarkable resistance against both the gram positive and gram negative bacterial strains (Table 1). The zones of inhibition for pristine and irradiated Gx-cl-poly(AA)-IA against *Bacillus subtilis* were found to be 18.82 ± 0.54 mm; 20.51 ± 0.47 mm, against *Salmonella enteritis* were found to be 13.2 ± 0.24 mm; 16.1 ± 0.25 mm, against *Staphylococcus aureus* were found to be 13.02 ± 0.74 mm; 14.7 ± 0.86 mm and against *Escherichia coli* were found to be 21.21± 0.23 mm; 25.24 ± 0.15 mm, respectively(Table 1; Figs. 6a-d).

Table 1: Zone of inhibition against different bacterial strains for Ag^{+9} irradiated sample.

Bacteria	**Zones of growth inhibition (mm)**			
	Sample	**Gx-cl-poly(AA)-IA**		
		Control	**Pristine**	**Irradiated**
Bacillus subtilis	**M**	48.51	18.82	20.51
	±SD	0.58	0.76	0.58
	±SE	0.31	0.54	0.47
Staphylococcus aureus	**M**	40.77	13.02	14.7
	±SD	0.64	1.01	1.25
	±SE	0.42	0.74	0.86
Salmonella enteritis	**M**	40.34	13.2	16.1
	±SD	0.65	0.27	0.34
	±SE	0.43	0.24	0.25
Escherichia coli	**M**	37.52	21.21	25.24
	±SD	0.58	0.32	0.26
	±SE	0.47	0.23	0.15

Where Control = Amoxicillin drug; M = Mean value; ±SD = standard deviation and ±SE = standard error

The cell wall of gram positive bacteria consists of peptidoglycan and teichoic acid which contributes towards its overall negative charge. Whereas, the cell wall of gram negative bacteria is composed of lipopolysaccharides generating negative charge on the surface of the bacterium. The membrane stability and charges on the surface of both the types of bacteria are balanced by the electrostatic interactions of these negative charges with divalent counter ions such as Mg^{2+} and Ca^{2+}. The bactericidal activity of synthesized hydrogels against *Bacillus subtilis*, *Staphylococcus aureus, Escherichia coli* and *Salmonella enteritis* was probably due to ion-exchange effect [39]. According to this effect, divalent counter ions responsible for balancing of negative charges on bacterial cell wall and providing structural stability were attracted by the COO^- moieties present abundantly on the synthesized graft co-polymer of polyacrylic acid with *Gum xanthan* and were exchanged with H^+ ions which further promoted instability and resulted into collapse of the bacterial cell membrane (Scheme 1) [39]. The intercellular pH of the bacterium reduces on exposure to test sample containing $–COO^-$ moieties and catalyzed the denaturation of essential proteins, DNA rupture and lysis of cell membrane was triggered. So, the zones of inhibition were clearly visible after incubation period representing the antibacterial characteristics of the synthesized sample [39]. Also, on irradiation of the test samples with Ag^{+9} SHIs the improved antibacterial activity was observed. This was probably due to the incorporation of the Ag^{+9} SHIs into the polymeric matrix upon irradiation which were released in moist environment and got exchanged with divalent counter ions (Mg^{2+}/ Ca^{2+}) responsible for stabilization of the negative charges onto the surface of the bacterium. Once the Ag^{+9} SHIs were attached to the bacteria it immediately inhibits the process of the bacterial growth due to its potential of cell destruction by interacting with thiol-containing proteins and DNA. It also stops cell division along with the destabilization of bacterial cell wall and cell membrane [40]. This imposed the bacterial death along with appearance of larger zone of inhibition in vicinity of the sample and confirmed the bactericidal activity of the SHI irradiated samples (Scheme 1).

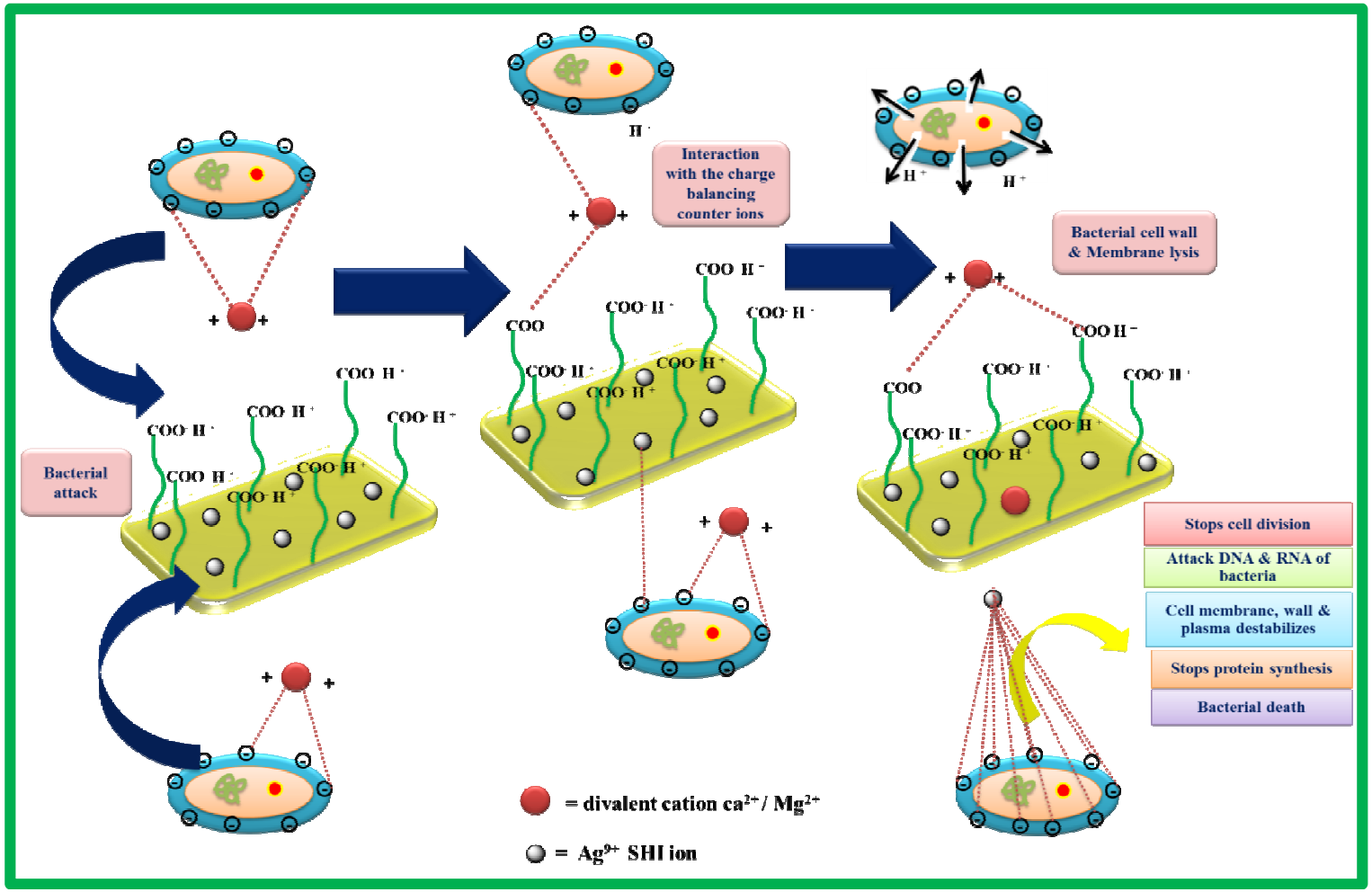

Scheme 1: Proposed mechanism for the interaction of bacterium with Ag^{9+} SHI ion irradiated *Gum xanthan* based hydrogels.

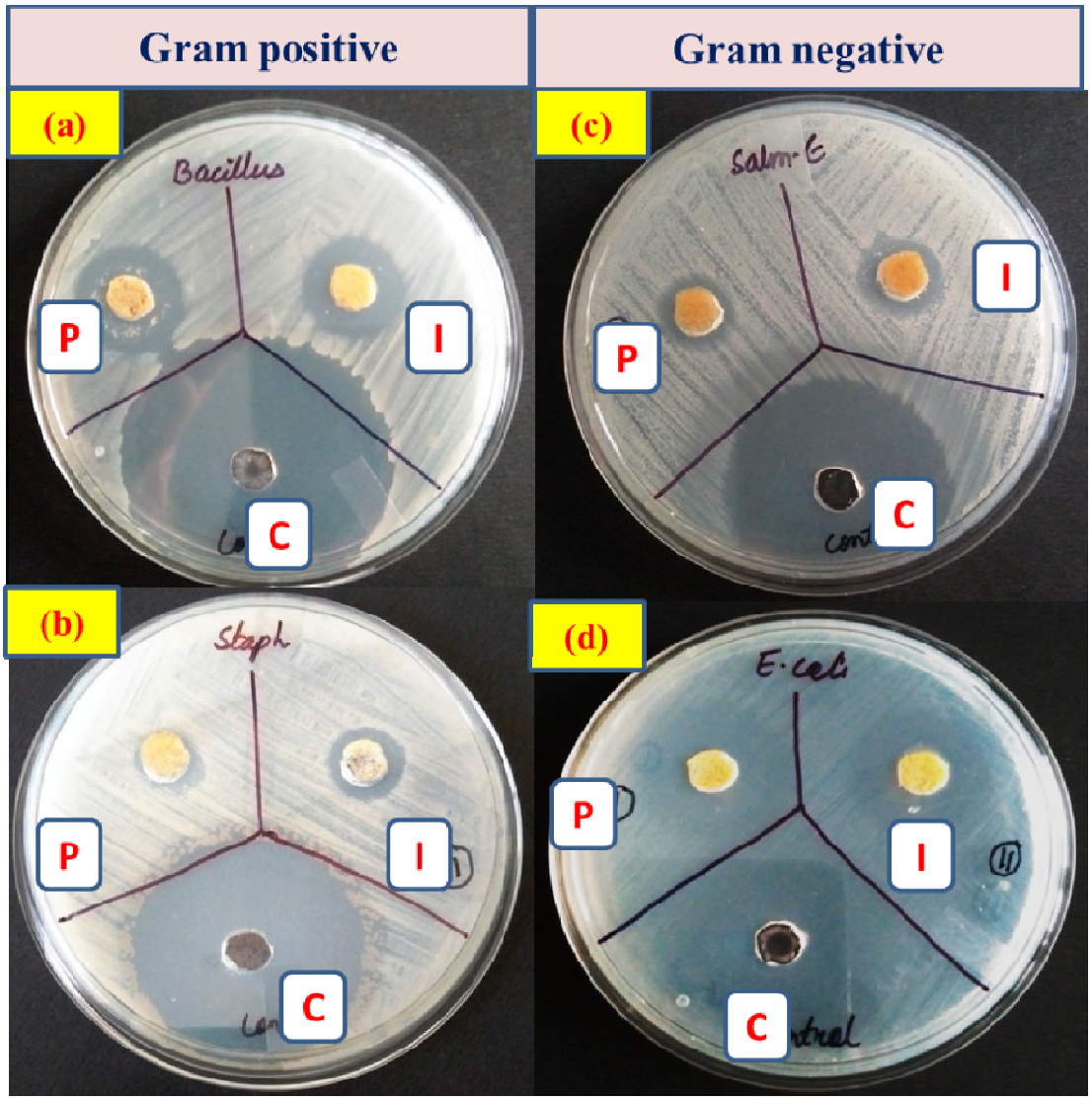

Figs. 6a-d. Antibacterial activity of pristine and Ag^{+9} SHI irradiated of Gx-cl-poly(AA)-IA against (a) *Bacillus subtilis*; (b) *Staphylococcus aureus*; (c) *Salmonella enteritis*; (d) *Escherichia coli.*

D. Dye sorption studies

The synthesized sample was found to be highly efficient in the removal of Aur-O dye. Auramine-O due to its cationic nature easily undergoes electrostatic interaction between positively charged active centers on the dye molecule and carboxylate moieties present abundantly on the adsorbent. Along with this interaction, it also undergoes dipole-dipole hydrogen bonding between the electronegative 'N' residue of dye molecule with the several –OH groups present on the hybrid backbone and grafted poly(acrylic acid) chains [34]. Further, cation-cation exchange also contributes towards the removal of auramine-O dye (Scheme 2) [41].

On irradiation of the samples with Ag^{+9} SHI, the percentage removal for the dye was studied under the conditions similar to that of pristine sample (100 mg sample in 30ppm 40 ml^{-1} of dyes solutions). It was found that evident increase in the sequestration potential of the adsorbent for Aur-O was observed. The percentage removal for Aur-O for pristine Gx-cl-poly(AA)-IA increases from 64.32% to 78.62% upon irradiation (Fig.7). The appearance of additional forces of attractions such as cation-cation exchange and electrostatic interactions due to impingement of the Ag^{+9} SHI ions in the pre-synthesized polymeric matrix were the probable reason behind the increase in the dye removal percentage (Scheme 4.2b) [42].

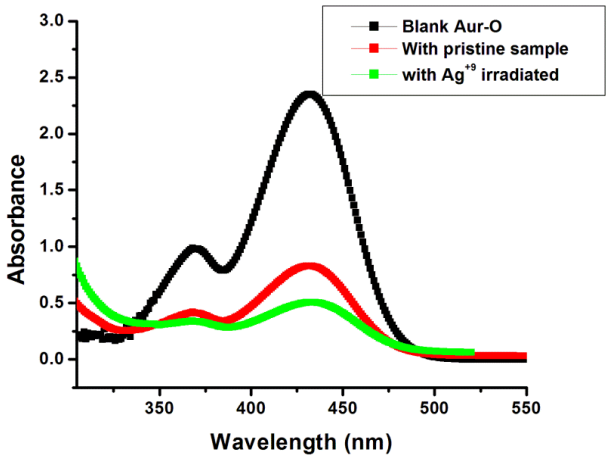

Fig. 7. Absorbance measurements for removal of Aur-O using pristine and Ag^{+9} irradiated Gx-cl-poly(AA)-IA.

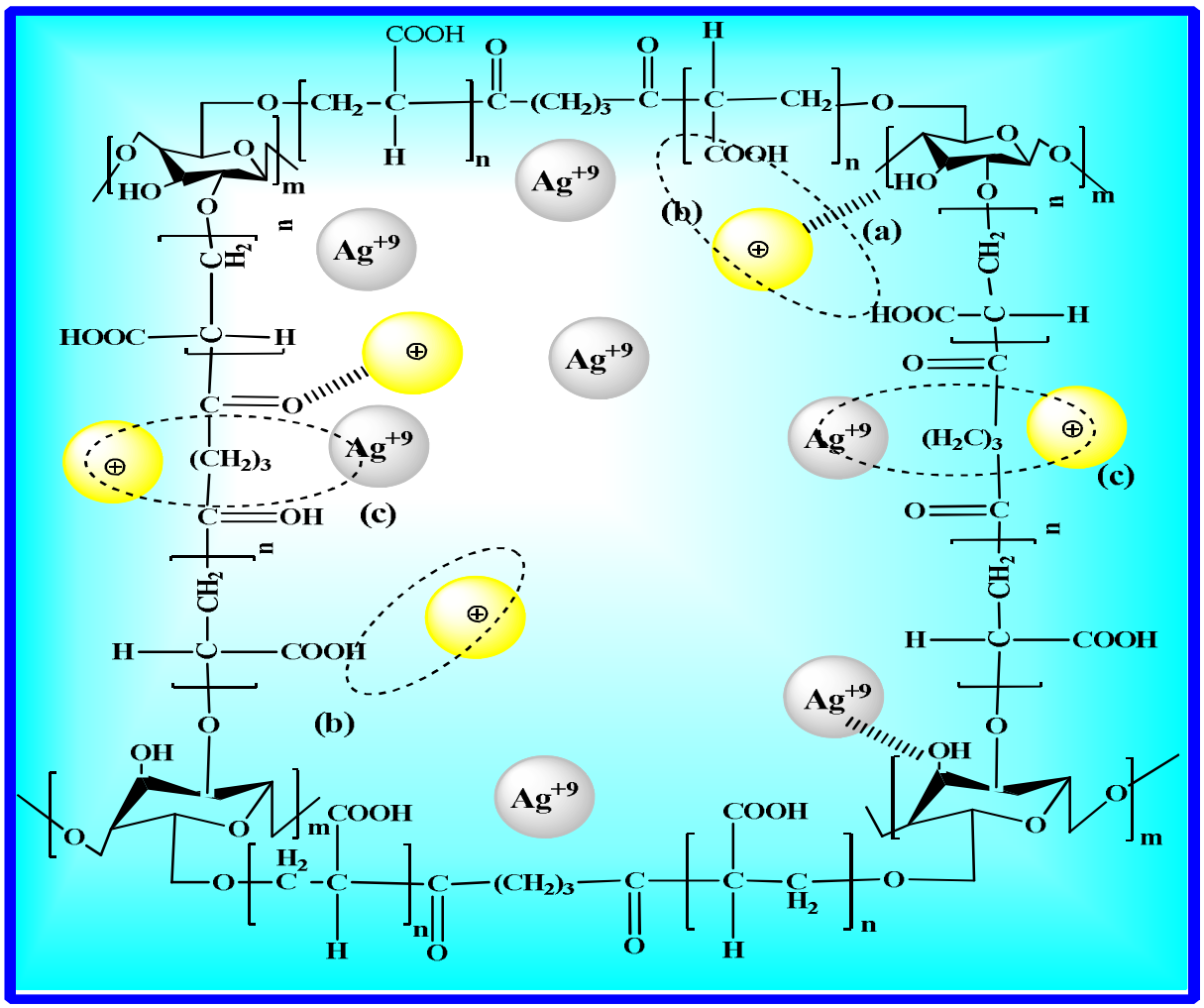

Scheme 2. Proposed mechanism for the removal of auramine-O using Ag^{+9} SHI irradiated hydrogels through (a) dipole-dipole hydrogen bonding; (b) ionic interactions; (c) cation-cation exchange**.**

CONCLUSION

Superabsorbent based on *Gum xanthan* grafted with polyacrylic acid was fabricated with maximum fluid uptake efficacy of 410.3%. Synthesized sample on irradiation with Ag^{+9} SHI depicted the remarkable change in the chemical and physical characteristics confirmed by various techniques. XRD spectra depicted increased crystallinity and crystallite size upon irradiation. FT-IR spectra showed the decrease in transmittance value along with shifting and disappearance of few peaks. Modified surface morphology with appearance of holes and fissures were clearly seen in the SEM micrographs. However, presence of Ag in EDX spectra confirmed its presence in the 3D network. Further investigation, confirmed that irradiated sample can be used effectively for the removal of auramine-O dye (78.62%) and also depicted enhanced anti-bacterial activity. So, the properties of biodegradable polymeric matrix can be altered successfully on irradiation to increase its utility in diverse field with good competence.

ACKNOWLEDGEMENTS

One of the author is extremely thankful to MHRD, New Delhi for providing fellowship for carrying out this research work. The author is also thankful to Instrumentation Center, IIT Roorkee, for characterization of the samples and DST-FIST New Delhi, for financial assistance for acquiring the FTIR and UV-Vis spectrophotometers at NIT Jalandhar. IUAC, New Delhi for providing beam irradiation facility. Department of Basic Sciences, Microbiology, UHF, Nauni, Solan, H.P, India for anti-bacterial studies.

REFERENCES

[1]. C. Chang, B. Duan, J. Cai, L. Zhang, Superabsorbent hydrogels based on cellulose for smart swelling and controllable delivery, *Eur. Polym. J.* **46** (2010) 92–100.

[2]. A. S. Hoffman, Hydrogels for biomedical applications, *Adv. Drug Delivery Rev.* **54** (2002) 3-12.

[3]. A. Pourjavadi , A.M. Harzandi, H. Hosseinzadeh, Modified carrageenan 3. Synthesis of a novel polysaccharide-based superabsorbent hydrogel via graft copolymerization of acrylic acid onto kappa-carrageenan in air, Eur. Polym. J. **40** (2004) 1363–1370.

[4]. H. Y. Cheung, K. T. Lau, T. P. Lu, D. Hui, A critical review on polymer-based bio-engineered materials for scaffold development, *Composites: Part B.* **38** (2007) 291–300.

[5]. M. Hamcerencu, J. Desbrieres, M. Popa, A. Khoukh, G. Riess, New unsaturated derivatives of Xanthan gum: Synthesis and characterization, *Polymer* **48** (2007) 1921-1929.

[6]. I. E. Raschip, E. G. Hitruc, A. M. Oprea, M. C. Popescu, C. Vasile, In vitro evaluation of the mixed xanthan/lignin hydrogels as vanillin carriers, *J. Mol. Struct.* **1003** (2011) 67–74.

[7]. R.C. Mundargi, S. A. Patil, T. M. Aminabhavi, Evaluation of acrylamide-grafted-xanthan gum copolymer matrix tablets for oral controlled delivery of antihypertensive drugs, *Carbohydr. Polym.* **69** (2007) 130–141.

[8]. I.W. Cottrell, K.S. Kang, P. Kovaca, In R. L. Davidson (Ed.), Handbook of water soluble gums and resins, New York: McGraw Hill, Kingsport Press, 1980.

[9]. M.C. Porte-Durrieu, C. Aymes-Chodur, N. Betz, C. Baquey, Development of "heparin-like" polymers using swift heavy ion and gamma radiation. I. Preparation and characterization of the materials, *J. Biomed. Mater. Res.* **52** (2000)119–127.

[10]. I.P. Jain and G. Agarwal, Ion beam induced surface and interface engineering, *Surf. Sci. Rep.* **66** (2011) 77–172.

[11]. L. Singh, K.S. Samra, Opto-structural characterization of proton (3 MeV) irradiated polycarbonate and polystyrene, *Radiat. Phys. Chem.* **77** (2008) 252-258.

[12]. T. Steckenreiter, E. Balanzat, H. Fuess, C. Trautmann, Chemical modifications of PET induced by swift heavy ions, *Nucl. Instr. Meth. B.* **131** (1997) 159-166.

[13]. V.K. Tiwari, D.K. Avasthi, P. Maiti, Swift Heavy Ion Induced Ordering and Piezoelectric β-phase in Poly(vinylidene fluoride), *ACS Appl. Mater. Interfaces.* **3**(2011) 1398–1401.

[14]. R. Singhal, D.C. Agarwal, Y.K. Mishra, S. Mohapatra, D.K. Avasthi, A.K. Chawla, R. Chandra, J.C. Pivin, Swift heavy ion induced modifications of optical and microstructural properties of silver–fullerene C60 nanocomposite, *Nucl. Instr. Meth. Phys. Res.* **267** (2009) 1349–1352.

[15]. H. J. Klasen, Historical review of the use of silver in the treatment of burns. *I. Early uses. Burns*. **26** (2000)117–130.

[16]. M. Yamanaka, K. Hara, J. Kudo, Bactericidal actions of a silver ion solution on Escherichia coli, studied by energy-filtering transmission electron microscopy and proteomic analysis, *Appl. Environ. Microbiol.* **71**(2005) 7589–7593.

[17]. Y.M. Mohan, K. Vimala, V. Thomas, K. Varaprasad, B. Sreedhar, S.K. Bajpai, K.M. Raju, Controlling of silver nanoparticles structure by hydrogel networks, *J. Colloid Interf. Sci.* **342** (2010) 73–82.

[18]. T. Jayaramudua, G. M. Raghavendraa, K. Varaprasad, R. Sadiku, K. Ramam, K. M. Raju, Iota-Carrageenan-based biodegradable Ag^0 nanocomposite hydrogels for the inactivation of bacteria, *Carbohydr. Polym.* **95** (2013) 188–194.

[19]. P. Jain and T. Pradeep, Potential of Silver Nanoparticle-Coated Polyurethane Foam as an Antibacterial Water Filter. *Biotechnol. Bioeng.* **90** (2005) 59-63.

[20]. D. H. K. Reddy and S. M. Lee, Application of magnetic chitosan composites for the removal of toxic metal and dyes from aqueous solutions, *Adv. Colloid Interface Sci.* 201–202 (2013) 68–93.
[21]. H. Tang, W. Zhou and L. Zhang, Adsorption isotherms and kinetics studies of malachite green on chitin hydrogels, *J. Hazard. Mater.* 209-210 (2012) 218–225.
[22]. B. D. C. Ventura-Camargo and M. A. Marin-Mor, Azo Dyes: Characterization and Toxicity – A Review, Textiles and Light *Industrial Science and Technology*. **3**(2013) 85–103.
[23]. I. D. Mall, V. C. Srivastava, N. K. Agarwal, Adsorptive removal of auramine-O: kinetic and equilibrium study, *J. Hazard. Mater.* **143** (2007) 386–395.
[24]. M. Vakili, M. Rafatullah, B. Salamatinia, A.Z. Abdullah, M.H. Ibrahim, K.B. Tan, Z. Gholami, P. Amouzgar, Application of chitosan and its derivatives as adsorbents for dye removal from water and wastewater: a review, *Carbohydr. Polym.* **113** (2014) 115–130.
[25]. G. Crini, Non-conventional low-cost adsorbents for dye removal: a review, *Bioresour. Technol.,* 2005, **97**, 1061–1085.
[26]. J. Sharma, Sukriti, P. Anand, V. Pruthi, A. S. Chaddha, J. Bhatia, B.S. Kaith, RSM-CCD optimized adsorbent for the sequestration of carcinogenic rhodamine-B: Kinetics and equilibrium studies, *Mater. Chem. Phys.* **196** (2017) 270-283.
[27]. V. Kumar, R.G. Sonkawade, A.S. Dhaliwal, High electronic excitation induced modifications by 100 MeV O^{7+} and 150 MeV Ni^{11+} ions in Makrofol KG polycarbonate film, *Nucl. Instr. Meth. Phys. Res.,* **287** (2012) 4–9.
[28]. Y. Ali, V. Kumar, R.G. Sonkawade, A.S. Dhaliwal. Effect of swift heavy ion beam irradiation on Au-polyaniline composite films, *Vacuum.* **90** (2013) 59-64.
[29]. B. S. Kaith, Sukriti, J. Sharma, T. Kaur, S. Sethi, U. Shanker, V. Jassal, Microwave‐assisted green synthesis of hybrid nanocomposite: removal of Malachite green from waste water, Iran. *Polym. J.* **25** (2016) 787-797.
[30]. K. Vimala, K.S. Sivudu, Y. M. Mohan, B. Sreedhar, K. M. Raju, Controlled silver nanoparticles synthesis in semi-hydrogel networks of poly(acrylamide) and carbohydrates: A rational methodology for antibacterial application, *Carbohydr. Polym.* **75** (2009) 463–471.
[31]. N. A. Ibrahim, W. M. Z. W. Yunus, F. A. Abu-Ilaiwi, M. Z. Ab Rahman, M. B. Ahmad, K. Z. M. Dahlan, Graft Copolymerization of Methyl Methacrylate onto Oil Palm Empty Fruit Bunch Fiber Using H_2O_2/Fe_2 as an Initiator, *J. Appl. Polym. Sci.* **89** (2003) 2233–2238.
[32]. V.D. Athawale, V. Lele, Graft copolymerization onto starch. II. Grafting of acrylic acid and preparation of it's hydrogels, *Carbohydr. Polym.* **35** (1998) 21-27.
[33]. G.R. Mahdavinia, A. Pourjavadi, H. Hosseinzadeh, M.J. Zohuriaan, Modified chitosan 4. Superabsorbent hydrogels from poly(acrylic acid-co-acrylamide) grafted chitosan with salt- and pH-responsiveness properties, *Eur. Polym. J.* **40**(2004) 1399–1407.
[34]. Sukriti, J. Sharma, V. Pruthi, P. Anand, A. P. S. Chaddha, J. Bhatia, B. S. Kaith, Surface response methodology–central composite design screening for the fabrication of a Gx-psy-g-polyacrylic acid adsorbent and sequestration of auramine-O dye from a textile effluent, *RSC Adv.* **6** (2016) 74300–74313.
[35]. J. Sharma, Sukriti, B. S. Kaith, M. S. Bhatti, Fabrication of Biodegradable Superabsorbent Using RSM Design for Controlled Release of KNO_3, *J. Polym. Environ.* (2017) 1-14.
[36]. A. Vij, A.K. Chawla, R. Kumar, S.P. Lochab, R. Chandra, N. Singh, Effect of 120 MeV Ag^{9+} ion beam irradiation on the structure and photoluminescence of SrS:Ce nanostructures, *Physica B.* **405** (2010) 2573–2576.
[37]. N.L. Singh, S. Shah, A. Qureshi, A. Tripathi, F. Singh, D.K. Avasthi, P.M. Raole, Effect of ion beam irradiation on metal particle doped polymer composites, *Bull. Mater. Sci.* **34** (2011) 81–88.
[38]. K. Hareesh, P. Sen, R. Bhat, R. Bhargavi, G.G. Nair, Sangappa, G. Sanjeev, Proton and alpha particle induced changes in thermal and mechanical properties of Lexan polycarbonate, *Vacuum* **91** (2013) 1-6.
[39]. G. Gratzl, S. Walkner, S. Hild, A.W. Hassel, H.K. Weber, C. Paulik, Mechanistic approaches on the antibacterial activity of poly(acrylic acid) copolymers, *Colloid. Surf. B.* **126** (2015) 98–105.
[40]. W. K. Jung, H.C. Koo, K.W. Kim, S. Shin, S. H. Kim, Y.H. Park, Antibacterial Activity and Mechanism of Action of the Silver Ion in *Staphylococcus aureus* and *Escherichia coli*, *Appl. Environ. Microbiol.* **74** (2008) 2171-2178.
[41]. S. Ghorai, A. Sarkar, M. Raoufi, A. B. Panda, H. Schonherr, S. Pal. Enhanced Removal of Methylene Blue and Methyl Violet Dyes from Aqueous Solution Using a Nanocomposite of Hydrolyzed Polyacrylamide Grafted Xanthan Gum and Incorporated Nanosilica, *ACS Appl. Mater. Interfaces.* **6** (2014) 4766–4777.
[42]. B.S. Kaith, R. Sharma, K. Sharma, S. Choudhary, V. Kumar, S.P. Lochab, Effects of O^{7+} and Ni^{9+} swift heavy ions irradiation on polyacrylamide grafted Gum acacia thin film and sorption of methylene blue, *Vacuum.* **111** (2015) 73-82.